Journal of
Composites Science

MDPI

Article

Research on the Nonlinear Confined Buckling Pressure of a Thin-Walled Metal Liner with an Ovality Defect Installed Inside the Composite Overwrapped Pressure Vessels

Fuwei Gu [1,*], Hu Xiao [1], Hao Wang [1], Zhiyang Chen [1], Kang Su [1], Zhiyi Tian [1], Xinpeng Li [1] and Yaguo Jin [2]

[1] School of Mechanical Engineering, Jiangsu University of Technology, Changzhou 213001, China; 2023655130@smail.jsut.edu.cn (H.X.); 2023655272@smail.jsut.edu.cn (H.W.); 2023655140@smail.jsut.edu.cn (Z.C.); 2024655305@smail.jsut.edu.cn (K.S.); 2024655117@smail.jsut.edu.cn (Z.T.); 2024655020@smail.jsut.edu.cn (X.L.)
[2] Jiangsu Ankura Intelligent Electric Co., Ltd., Changzhou 213001, China; 2022655211@smail.jsut.edu.cn
* Correspondence: gufuwei@jstu.edu.cn

Abstract

Composite overwrapped pressure vessels (COPVs) have become the core unit for high-pressure hydrogen storage and transportation. However, excessive autofrettage pressure could induce unilateral buckling damage of the metal liner because of large rebound compressive stress induced by large plastic deformation in the depressurization stage. When the liner contains initial defects, its critical unilateral buckling pressure would be further reduced. In this paper, a critical buckling pressure calculation formula was established by finite element analysis and theoretical derivation. Firstly, the classical theoretical calculation models and research methods were analyzed and discussed. Then, by discussing the key influencing parameters, a semi-empirical calculation formula of nonlinear confined buckling pressure of a metal liner with ovality defects was established. Finally, the proposed semi-empirical formula was used to predict the critical internal pressure of a Type-III COPV, and the predicted value was compared with the experimental result. The predicted result was higher than the experimental result and the error range was −2.8%~−23%. The proposed semi-empirical formula of nonlinear confined buckling could provide theoretical support for designing the autofrettage pressure of Type-III COPVs and help to reduce the uncertainty and repeated test cost in the design process.

Keywords: COPVs; thin-walled metal liner; nonlinear confined buckling; elastic buckling; ovality defect; finite element analysis

Academic Editor: Dimitrios Tzetzis

Received: 18 July 2025
Revised: 14 August 2025
Accepted: 26 August 2025
Published: 3 September 2025

Citation: Gu, F.; Xiao, H.; Wang, H.; Chen, Z.; Su, K.; Tian, Z.; Li, X.; Jin, Y. Research on the Nonlinear Confined Buckling Pressure of a Thin-Walled Metal Liner with an Ovality Defect Installed Inside the Composite Overwrapped Pressure Vessels. *J. Compos. Sci.* **2025**, *9*, 480. https://doi.org/10.3390/jcs9090480

1. Introduction

Hydrogen energy is regarded as one of the most promising secondary energy sources in the 21st century because of its advantages of zero pollution, renewability, storability and wide sources [1]. At present, the composite overwrap pressure vessel (COPV) has become the core equipment for hydrogen gas storage and transportation [2,3]. For a COPV subjected to internal pressure loading, the metal liner—due to its relatively low yield strength—often yields before the fiber reinforcement layer fails. This results in circumferential and axial plastic deformation in the liner while the fiber winding layer remains in the elastic deformation stage. Upon pressure relief, the elastic recovery of the fiber overwrap induces an equivalent external pressure on the expanded liner, placing the metal liner in compression and the fiber layer in tension under zero-pressure conditions.

Consequently, when the vessel is repressurized to working pressure, the liner operates at a reduced stress level, thereby enhancing its fatigue life. This stress redistribution mechanism is the fundamental principle behind overpressure autofrettage technology.

During the overpressure autofrettage process, if the equivalent external pressure induced by the elastic recovery of the fiber reinforcement layer exceeds a critical threshold, the inner liner may experience inward collapse. Upon repressurization, the collapsed section is forced back into position. This cyclic buckling and rebuckling behavior during repeated loading–unloading operations can lead to premature fatigue failure of the liner. Jahromi et al. [4] investigated the stress and strain distribution in Type III COPV liners resulting from autofrettage and developed a theoretical model for residual stress assessment. Hu et al. [5] established a finite element model about the autofrettage of the composite cylinder's liner with different defects. By simulating the autofrettage process, it was found that the autofrettage of the liner can significantly improve the fracture resistance of the pressure vessel. Li et al. [6] studied the influence of different stacking sequences of winding layers on the bursting pressure, and established a model by FEM to predict the bursting pressure through the progressive damage model. Wu et al. [7] determined the optimum range of autofrettage pressure through FEM, and discussed the influence of self-strengthening pressure, metal lining thickness and fiber thickness on the fatigue life of vessels. According to the principle of minimum potential energy, Li et al. [8] derived the elastic analytical solution of a thin-walled liner with initial deflection, ovality and other defects. At present, the relevant design standards do not put forward corresponding design criteria for the buckling damage of the liner. The standards mainly focus on strength, fatigue life and fiber utilization (fiber stress ratio), which increases the uncertainty in the design process of COPVs. Therefore, predicting the critical buckling pressure of COPVs liners has an important influence on the life and reliability.

Due to the circumferential constraint of the carbon fiber layer, the instability direction of the metal liner is toward the inside, which belongs to the research category of confined buckling or instability. Confined buckling/confined instability refers to the phenomenon that the stressed components cannot deform freely due to the outer wall's constraint. Such problems often occur in buried pipelines [9], steel lining shells of nuclear reactors [10], pipeline liners [11] and anti-corrosion linings of urea synthesis towers [12]. Different from the free deformation of single thin, in order to achieve the minimum energy balance, the inner liner constrained by the outer wall usually exhibits the deformation characteristics of one-way buckling to the inside. Usually, in order to preventing leakage or corrosion, the liner is mainly made of thin-walled plastic or metal materials, and it is generally considered that the plastic liner mainly buckles elastically. The metal liner usually reflects the elastic–plastic buckling. With the deepening of research, the initial defects of the liner also have an important influence on its buckling, and scholars have carried out a lot of research work on the restrained buckling of the liner.

In this paper, as shown in Figure 1, a calculation model was established by finite element analysis and theoretical derivation. Then, the key influencing parameters were discussed, and a semi-empirical formula for predicting the critical buckling pressure of the liner was proposed. To verify the reliability of a proposed prediction model, the predicted value was compared with the experimental result.

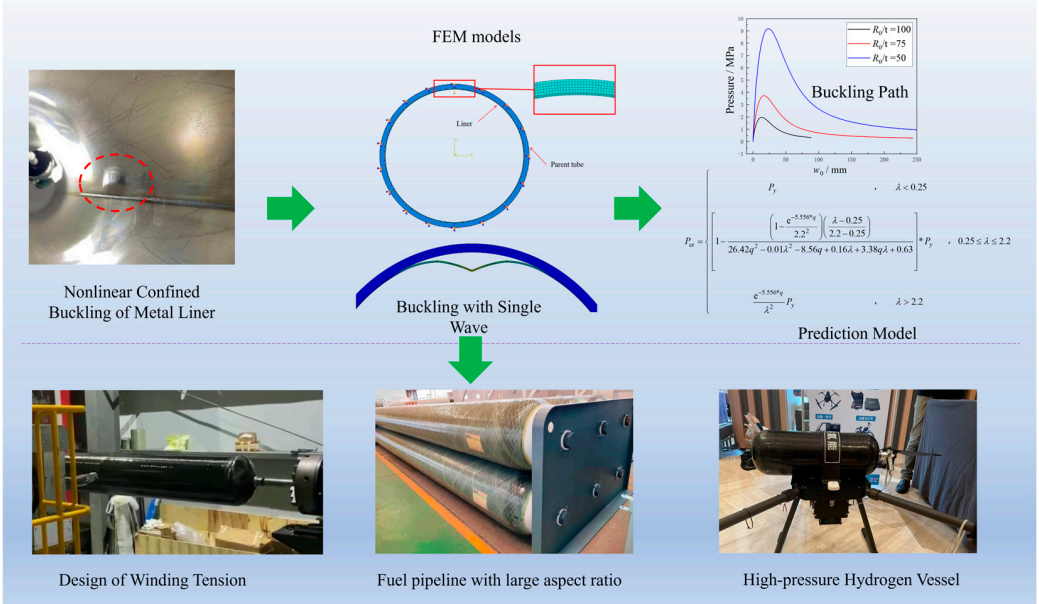

Figure 1. General drawing of the research logic and the typical application.

2. Theoretical Calculated Models of Elastic and Nonlinear Confined Buckling of Liner

2.1. Elastic Confined Buckling Theory Calculated Models

Elastic confined buckling means that the stress–strain relationship of the metal liner always maintains a linear elastic state, so the theoretical objects are usually very thin metal plates, shells and plastic liners. There are two main research methods for elastic confined buckling for thin-walled liners. One is the thin-walled confined buckling theory of short cylindrical shells, and the other is the circular confined buckling theory of long cylindrical shells.

The confined buckling theory of thin shells focuses primarily on the critical instability behavior of short cylindrical structures supported by rigid outer walls or elastic media. Under rigid outer wall conditions, the theoretical approach for analyzing confined buckling in such shells bears resemblance to the computational procedure for free buckling of thin shells. Leveraging the principle of minimum potential energy, the simplified Donnell deformation equation serves to compute critical loads encompassing both axial compression and external pressure. Meanwhile, the Donnell nonlinear large-deflection deformation equation is employed to investigate the post-buckling behavior of thin shells that exhibit initial deflections [13]. Different from free buckling, the confined buckling deflection function of thin shells must reflect that the buckling waveform is limited by circumferential and longitudinal constraint. For example, Lin Yantian [14] uses three displacement functions of radial direction, tangential direction and axial direction to represent three modes of axial unilateral buckling, circumferential unilateral buckling and mixed unilateral buckling. Then, the Rayleigh–Ritz energy method was applied to calculate the confined buckling of the thin-walled shell under external pressure. Moore et al. [15] used Fourier series to expand the buckling displacement of the ring, and obtained a buckling eigenvalue of the corrosion-resistant thin-walled metal liner under vacuum or thermal stress by the Sanders nonlinear deflection equation.

For long cylindrical shells, what the researchers detected through experiments [16–19] was the circumferential inward single buckling waveform of the liner, which constitutes a distinctive buckling mode characteristic of thin-walled confined liners. Therefore, based on this single-wave buckling mode of long cylindrical shells, Glock [20] derived the theoretical

calculation formula of critical elastic buckling pressure of the thin-walled liner in rigid body by using the ring theory which is based on the plane strain assumption. Glock obtains the circumferential strain energy U_ε of the buckling and unbending parts of the whole ring, the bending strain energy U_k of the buckling part of the ring, and the work W performed by external pressure, thus the total potential energy Π of the liner is shown in Equation (1).

$$\Pi = U_k + U_\varepsilon - W \tag{1}$$

In view of the universality elastic confined buckling with single wave mode, Glock further puts forward the radial deflection curve equation about w, shown in Equation (2), in which the variables of w_0 and ϕ_0 are the maximum deflection and the maximum deflection boundary, respectively.

$$w = w_0 \cos^2 \frac{\pi\phi}{2\phi_0} \quad ; \quad 0 \le \phi \le \phi_0 \tag{2}$$

Substituting Equation (2) into Equation (1) and based on the principle of minimum potential energy, the classical Glock critical external pressure calculation formula can be finally obtained, as shown in Equation (3), in which the variables of E, ν, t and R are the elastic modulus, Poisson's ratio, wall thickness and mid-plane radius of the liner, respectively.

$$P_{\text{Glock}} = \frac{E}{1-\nu^2}\left(\frac{t}{2R}\right)^{2.2} \tag{3}$$

For an ideal long cylindrical shell, the classical Glock's formula exhibits high predictive accuracy and has gained widespread acceptance. Building upon the derivational procedure of Glock's critical formula, Boot [21] put forward the hypothesis of double-wave elastic buckling, which extended the classical Glock's theory. Li et al. [22] derived the theoretical calculation formula of critical external pressure for elastic confined buckling with uneven thickness liner, while Omara [16] and Jing Yingdong [11] derived the theoretical calculation formula for ovality liner under rigid outer wall. Therefore, Glock's critical buckling external pressure formula has been widely adopted and has established itself as a foundational basis for numerous theoretical investigations.

2.2. Nonlinear Confined Buckling Theoretical Calculated Models of Confined Thin-Walled Liner

For metal liners, material yielding behavior typically takes place prior to elastic buckling, resulting in a nonlinear response throughout the entire buckling process. Consequently, elastic theory is no longer applicable.

As a first approximation, Montel [23] proposed that the critical external pressure corresponds to the pressure causing the metal liner to undergo initial yielding. Based on this concept, a semi-empirical formula was developed by incorporating Timoshenko's deflection solution [24] and experimental findings [25], as presented in Equation (4). Within this formula, denotes the yield strength of the metal liner, while the influences of the liner's initial deflection and initial clearance on the nonlinear critical buckling pressure are accounted for.

$$P_{\text{M}} = \frac{14.1\sigma_y}{(2R/t)^{1.5}[1 + 1.2(\delta_0 + 2g)/t]} \tag{4}$$

Based on numerical simulation findings, Vasilikis et al. [26] incorporated the plastic hinge into the buckling analysis for confined metal liners, and considered that the moving plastic hinge and the static plastic hinge in the middle section were generated. It was assumed that the rest parts except the plastic hinge were rigid and plastic, and then the critical external pressure for nonlinear buckling was obtained according to the fact that the plastic work was equal to the external work. However, this theory fails to account for the

additional energy required for the plastic hinge to move at both ends, resulting in a certain discrepancy between theoretical predictions and experimental observations.

In addition, as the upper limit of nonlinear critical buckling pressure, based on the Mises strength criterion, the critical pressure at which the entire wall thickness of the metal liner enters the yield state also plays a significant role in deriving empirical formulas, as presented in Equation (5).

$$P_y = 2\frac{\sigma_y}{\sqrt{1-\nu+\nu^2}}\left(\frac{t}{2R}\right) \tag{5}$$

2.3. Confined Buckling Analysis Method of Liners with Defects

2.3.1. Elastic Confined Buckling Theory with Initial Defects

In the process of engineering application, the thin-walled liner structure will produce some defects due to some objective reasons during installation and use. According to the characteristics of these defects, the researchers combed and summarized that the main defects of the liner are initial deflection, initial clearance, ovality shape defects and uneven wall thickness and so on. Based on the ring theory and finite element calculation model, researchers have carried out a lot of research on these defects, respectively. In the early theoretical research, it is usually difficult to obtain the theoretical formula for calculating the critical external pressure of a thin-walled liner with initial defects. Zhang [27] used Equation (4) to predict the critical buckling pressure of the metal liner of the COPV. The theoretical buckling pressure of S30408 stainless steel liner was about 14.4 MPa, while the experimental results showed that the critical buckling pressure was between 15~18 MPa, and the error range between theoretical calculation results and experimental measurement outcomes was 4–20%. Primary factors contributing to these errors include insufficient accuracy of experimental measurements, failure to consider the compression effect of the initial winding tension of the fiber winding layer on the liner, the influence on the bond strength of the liner and the initial ovality defect of the metal liner.

Benefiting from the development of the technology of FEM, El-Sawy et al. [28] first adopted finite element technology to establish a finite calculation model with various defects. According to the calculation results, the corresponding semi-empirical expressions of attenuation coefficients are put forward, and these attenuation coefficients usually have high calculation accuracy and are widely recognized. Therefore, in order to facilitate engineering calculation, most of the proposed calculation models are empirical formulas and semi-empirical formulas [29–34]. For example, when Omara et al. [16] studied the influence of ovality defects, some secondary factors were ignored, and some unknown parameters were linearized according to the experimental results, so a semi-empirical calculation formula was obtained.

2.3.2. Nonlinear Confined Buckling Theory with Initial Defects

Because the buckling process of metal liner is usually accompanied by plastic hinge, the whole buckling process is nonlinear. When considering the initial defects of metal liner, it is more difficult to obtain the critical buckling internal pressure of metal liner by theoretical research. At present, there is little research work on this kind of problem, and the existing research works tend to adopt the method of FEM [35,36].

For Type-III COPV, among several common defects of metal liner, ovality defect is the most easily overlooked and difficult to be accurately measured, and the influencing mechanism has not been found yet. Based on the above research status, this paper focuses on the influence of ovality defects on the nonlinear confined buckling of thin-walled metal liner installed inside the composite overwrapped pressure vessel. Firstly, combined with finite element analysis method, The predictive accuracy of several empirical formulas for elastic buckling with ovality defects is evaluated and compared. Building upon this

analysis, an empirical formula for nonlinear confined buckling involving ovality defects is developed. Leveraging the deformation mechanism of composite overwrapped pressure vessels, a theoretical model for calculating the critical buckling pressure of thin-walled metal liners with ovality defects is established, with theoretical calculation results and experimental data subsequently compared and analyzed.

3. Confined Buckling of Thin-Walled Metal Liner with Ovality Defects

According to the above discussion, in the design process, there are few reports on the nonlinear confined buckling of thin-walled metal liners with ovality defects. For the composite overwrapped pressure vessel, the COPV's inner vessel is usually formed by cold drawing, extrusion or cold and hot reverse extrusion molding, and then it is prepared by forging, spinning or welding techniques to form domes at both ends of the cylinder. These processing techniques require extremely high stability of the system, and the inner is very prone to some initial damage, such as ovality deformation, local depression, surface scratches and other initial defects.

Therefore, in this section, firstly, the prediction accuracy of various theoretical formulas about elastic confined buckling of the inner with ovality defects is compared with the finite element calculation results. On the basis of the existing empirical formulas of elastic confined buckling, the influence of ovality defects on nonlinear confined buckling of liner is discussed through the finite element calculation model, and a simple and effective empirical formula of nonlinear confined buckling with ovality defects was proposed.

3.1. Calculation Model of Elastic Confined Buckling of Thin-Walled Liner with Ovality Defect

3.1.1. Finite Element Calculation Model and Basic Assumptions

This paper discusses the influence of different ovality defects and material nonlinearity on the confined buckling of the liner through a two-dimensional plane finite element calculation model. The two-dimensional plane finite element model described in this paper is based on the following assumptions:

(1) Assuming that the pipeline is infinitely long (the length-diameter ratio is greater than 6) [36], ignoring the axial deformation of the liner, the buckling deformation of the pipeline's liner satisfies the assumption of plane strain condition.
(2) It is assumed that the liner bears uniform annular outward pressure.
(3) The interface between the liner and the outer tube is smooth and frictionless, so there is no shear stress to do work during the buckling of the liner.

The above basic assumptions are similar to those of Glock's elastic buckling theory, and the finite element model is a two-dimensional ring under the condition of plane strain. Based on the cross sections of the inner and the outer base pipe, the two-dimensional plane finite element calculation model is shown in Figure 1. In order to meet the basic assumptions of Glock theory, 8-node reduced integral plane strain element (CPE8R) is adopted for both the liner and the base pipe. In order to meet the assumed conditions, the contact surface between the liner and the base pipe adopts frictionless normal and tangential contact pair attributes. The number of circumferential grids of the liner is 500, and the number of grids in the thickness direction of the liner is 3; The number of circumferential grids in the base pipe is 400, and the number of grids in the thickness direction is 5, among which the number of circumferential grids of inner or base pipe is not fixed, which plays a great role in the convergence of the model. Debugging the number of circumferential grids is helpful to calculate the convergence of the model.

It is worth noting that this model usually has no ellipse or other defects, and the single-wave buckling mode is difficult to occur when the liner is subjected to external pressure by using Riks Algorithm iterative control technology. However, when the ovality

defect is large, it is very easy for the ovality liner to buckle at two positions of the short semi-axis at the same time, and the strain energy dissipated by double-wave buckling is greater than that of single-wave buckling. Therefore, the calculation results of single-wave buckling mode are conservative. In order to obtain single-wave, there are two steps in the ABAQUS models and the implicit analysis step is added before the Riks analysis step. For implicit analysis step, a concentrated force with the size of 0.01 N is applied to the corresponding node of the short semi-axis of the ovality liner, as shown in Figure 2. For the Riks analysis step, a uniform annular outward pressure is applied to the corresponding node of the short semi-axis of the liner, and the concentrated force is removed, so that the initial disturbance caused by the concentrated force can be transmitted to Riks analysis step. Non frictional contact is set between the inner and the base pipe. At the same time, the Y-direction displacement of the corresponding node is output, which is used to record the equilibrium path of the liner in the buckling process.

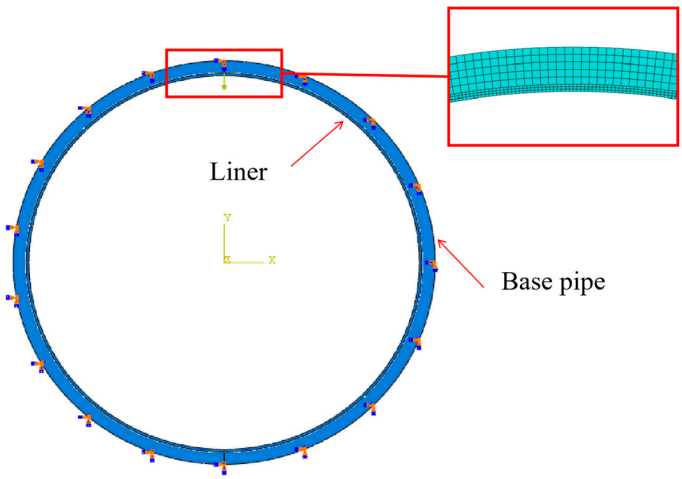

Figure 2. Two-dimension plane finite element calculation model of confined instability of liner.

For the composite overwrapped pressure vessel, the buckling of the inner liner is instantaneous, and the circumferential pressure between the liner and the base pipe is caused by the circumferential contraction of the fiber layer. The ultimate buckling deformation of the liner will keep the whole system at the lowest energy state. Through a large number of finite element models, it can be found that the Riks analysis step is difficult to converge when the stiffness and thickness of the base pipe are small. However, when the modulus of the base pipe is one tenth of that of the liner, it has little influence on the buckling damage of the liner [26]. Therefore, this paper holds that the critical buckling pressure of the liner is not affected by the interaction between the liner and the base pipe during the buckling deformation. In the finite element model, only the buckling deformation of the liner in the rigid base pipe is considered, so this goal can be achieved by imposing full constraints on the base pipe, shown as Figure 2.

This section takes the steel liner as the research object, and its elastic modulus is 210,000 MPa and Poisson's ratio is 0.3. Firstly, a finite element calculation model without ovality defects is established. In the model, the radius R of the steel liner is 500 mm, and R/t is 100, where t is the wall thickness of the steel liner. As shown in Figure 3a,b, the elastic buckling process of the steel liner mainly includes three stages. First, under the action of internal pressure, the steel liner generates uniform compression deformation in the arc near the initial disturbance point, and the initial disturbance point generates radial displacement of w_0 towards the center of the circle. At this time, the region still has a certain curvature, and the curvature of the liner remains basically unchanged under the support of

the base pipe. However, when the external pressure continues to increase, the arc near the initial disturbance point begins to appear as a platform segment, at this time, the rigidity of the arc against external pressure deformation is reduced to the minimum, so the liner enters the second stage. As can be seen from Figure 3b, this stage reaches the critical buckling state with the highest pressure, but a slight increase in external pressure can break this balance, leading to the third stage of collapse of the liner, which is characterized by a large concave deformation of the liner and the release of strain energy to maintain a new one.

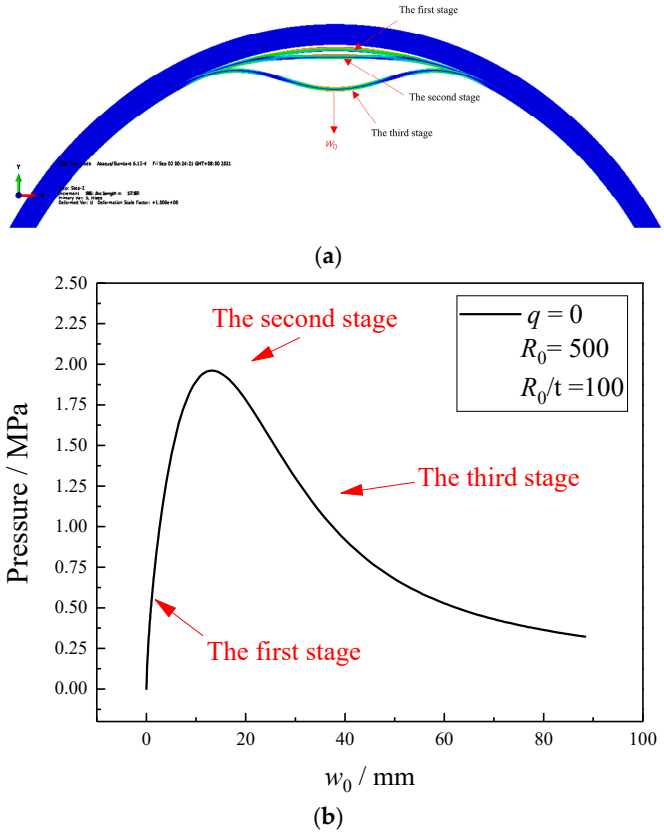

Figure 3. Instability process and buckling equilibrium path of liner. (**a**) Instability process of liner, (**b**) Buckling equilibrium path of liner.

Further, three finite element calculation models with R/t of 100, 75 and 50 with different diameter–thickness ratios are established. The buckling equilibrium paths of the three calculation models are shown in Figure 4. With the increase of wall thickness, the critical pressure of the inner tank arc also increases. Among them, the error between the maximum critical buckling pressure of the three models and Glock's elastic confined buckling theory results is shown in Table 1, and the maximum error is 1.95%. Therefore, Glock elastic buckling theory formula based on plane strain assumption has high calculation accuracy.

Table 1. Applications of electrospun separators and interlayers in lithium–sulfur batteries.

R_0 (mm)	R_0/t	q	P_{max} (MPa)	P_{Glcok} (MPa)	Error
500	100	0	1.961	2	1.95%
500	75	0	3.723	3.765	1.1%
500	50	0	9.192	9.187	−0.54%

Note: When R/t is 75 and 50, the stiffness of the liner increases, and the magnitude of concentrated force in the finite element calculation model is 0.02 N and 0.03 N, respectively, to generate the initial disturbance that induces single-wave buckling.

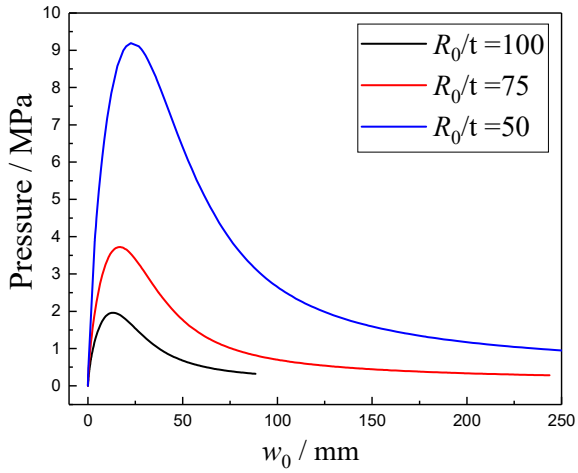

Figure 4. Buckling equilibrium path of liner with different diameter thickness ratio.

3.1.2. Calculation Results and Discussion of Elastic Confined Buckling with Ovality Defects

Based on the above finite element calculation model, the influence of ovality on elastic buckling is discussed. In order to express the degree of ovality deformation of pipes, the concept of ovality q defined in reference [28] is introduced in this paper, as shown in Equation (6).

$$q = \frac{R-b}{R} \quad \text{or} \quad q = \frac{a-R}{R} \quad \text{or} \quad q = \frac{a-b}{a+b} \tag{6}$$

Among them, a is the long semi-axis of the ellipse, b is the short semi-axis of the ellipse, and R represents the radius of the same circle as ellipse circumference, $R = \frac{a+b}{2}$; In this paper, the simplified calculation formula of ellipse circumference is $C_{\text{ellipse}} = \pi(a+b)$. When $b/a > 0.885$, the error between the calculation result of this ellipse circumference formula and the actual ellipse circumference is less than 0.001. Therefore, this simplified formula can achieve high engineering calculation accuracy.

When the liner has ovality defects, the closed calculation formula of the critical buckling pressure of the ovality liner cannot be deduced theoretically, which is very unfavorable for engineering application. Therefore, the main method adopted at present is to propose an attenuation coefficient C related to defects such as ellipses, local depressions and initial gaps on the basis of Glock theoretical formula to quantitatively describe the influence of defect size parameters on the critical buckling pressure, as shown in Equation (7).

$$P_{\text{cr}} = C * P_{\text{Glock}} = C * \frac{E}{1-\nu^2}\left(\frac{t}{2R_0}\right)^{2.2} \tag{7}$$

When the liner only has ovality defects, there are currently four empirical expressions of attenuation coefficient C related to ovality defects, as shown in Table 2.

Table 2. Empirical calculation formula of different attenuation coefficients related to ovality defects.

Attenuation Coefficient $C/(P_{\text{cr}}/P_{Glock})$	Formula Source
$(1+q)^{-\frac{8}{5}}(1-q)^{-\frac{1}{5}}$	Chicurel [37]
$\left[(1-q)/(1+q)^2\right]^3$	ASTM F1216-93 [38]
$e^{-5.556*q}$	Vasilikis [35]
$\left[1-\left(3q-q^3\right)\times\left(\frac{4\times q}{\pi}-2q+1\right)\right]^{1.8}$	Omara [16]

In order to compare the prediction accuracy of these four empirical coefficients, referring to the finite element model in Section 3.1.1, this paper established several groups of finite element calculation models for liners with R = 100, R/t = 150, 100 and 50, respectively, in the range of defects with ovality of q = 0~0.1. The ratio between the finite element critical buckling pressure calculation result $P_{cr}(oval)$ and the Glock buckling theory result $P_{Glcok}(circle)$ of the circular liner with the same circumference as the ovality liner is shown in Tables 3–5. It can be found that with the increase of ovality, the critical load decreases gradually, and the $\frac{P_{cr}(oval)}{P_{Glcok}(circle)}$ value of different R/t liners has little difference under the same ovality.

Table 3. Critical buckling attenuation coefficient under different ovality defects (R/t = 150).

q	$R = \frac{a+b}{2}$	R/t	$P_{cr}(oval)$ (MPa)	$P_{Glcok}(circle)$ (MPa)	$C = \frac{P_{cr}(oval)}{P_{Glcok}(circle)}$
0	500	150	0.801	0.819	0.978
0.01	500	150	0.759	0.819	0.927
0.02	500	150	0.718	0.819	0.877
0.03	500	150	0.681	0.819	0.831
0.04	500	150	0.646	0.819	0.789
0.05	500	150	0.613	0.819	0.748
0.06	500	150	0.581	0.819	0.709
0.07	500	150	0.551	0.819	0.673
0.08	500	150	0.522	0.819	0.637
0.09	500	150	0.496	0.819	0.606
0.1	500	150	0.470	0.819	0.574

Table 4. Critical buckling attenuation coefficient under different ovality defects (R/t = 100).

q	$R = \frac{a+b}{2}$	R/t	$P_{cr}(oval)$ (MPa)	$P_{Glcok}(circle)$ (MPa)	$C = \frac{P_{cr}(oval)}{P_{Glcok}(circle)}$
0	500	100	1.961	2	0.981
0.01	500	100	1.861	2	0.931
0.02	500	100	1.765	2	0.883
0.03	500	100	1.674	2	0.837
0.04	500	100	1.587	2	0.794
0.05	500	100	1.508	2	0.754
0.06	500	100	1.43	2	0.715
0.07	500	100	1.357	2	0.679
0.08	500	100	1.287	2	0.644
0.09	500	100	1.221	2	0.611
0.1	500	100	1.159	2	0.580

Table 5. Critical buckling attenuation coefficient under different ovality defects (R/t = 50).

q	$R = \frac{a+b}{2}$	R/t	$P_{cr}(oval)$ (MPa)	$P_{Glcok}(circle)$ (MPa)	$C = \frac{P_{cr}(oval)}{P_{Glcok}(circle)}$
0	500	50	9.192	9.187	1.00
0.01	500	50	8.74	9.187	0.951
0.02	500	50	8.29	9.187	0.902
0.03	500	50	7.84	9.187	0.853
0.04	500	50	7.453	9.187	0.811
0.05	500	50	7.08	9.187	0.771
0.06	500	50	6.69	9.187	0.728
0.07	500	50	6.34	9.187	0.690
0.08	500	50	6.03	9.187	0.656
0.09	500	50	5.727	9.187	0.623
0.1	500	50	5.364	9.187	0.584

By comparing the sizes of the four attenuation coefficients shown in Table 2 under different ovality defects with the finite element calculation results in Tables 4–6, as shown in Figure 5, it can be observed that, The size of R/t has a certain impact on the size of $C = \frac{P_{cr}(oval)}{P_{Glcok}(circle)}$, but the impact is relatively low. Although the attenuation coefficient proposed by Khaled M. El-S [28] did not take this factor into account, from a conservative perspective, Khaled M. El-S [28] takes the lower limit of $\frac{P_{cr}(oval)}{P_{Glcok}(circle)}$ with respect to the R/t curve, which makes the calculation results biased towards conservatism. However, overall, the attenuation coefficients related to ovality proposed by Khaled M. El-S [28] and Omara [16] have higher prediction accuracy. Considering that the attenuation coefficient expression proposed by Khaled M. El-S [28] is relatively simple and convenient, this paper intends to refer to the empirical formula for elastic confined buckling of metal liners containing ovality defects shown in Equation (8). to provide support for the study of elastic–plastic buckling of metal liners in the following text.

Table 6. Size of dependent parameters of η under different parameter conditions.

q	R/t	σ_y/E	σ_y (MPa)	P_y (MPa)	P_{Glock} (MPa)	λ	P_{max} (MPa)	η
0	25	0.0014	294	13.231	42.213	0.560	11.339	1.134
0.01	30	0.00142	298.2	11.183	28.265	0.629	8.491	1.539
0.02	35	0.00144	302.4	9.721	20.135	0.695	6.624	1.713
0.03	40	0.00146	306.6	8.624	15.010	0.758	5.297	1.795
0.04	45	0.00148	310.8	7.771	11.584	0.819	4.339	1.813
0.05	50	0.0015	315	7.088	9.187	0.878	3.584	1.819
0.06	55	0.00152	319.2	6.530	7.449	0.936	2.988	1.809
0.07	60	0.00154	323.4	6.064	6.151	0.993	2.517	1.785
0.08	65	0.00156	327.6	5.670	5.158	1.048	2.145	1.750
0.09	70	0.00158	331.8	5.333	4.382	1.103	1.834	1.715
0.10	75	0.0016	336	5.040	3.765	1.157	1.574	1.677
0.05	80	0.00162	340.2	4.784	3.267	1.210	1.755	1.524
0.05	85	0.00164	344.4	4.559	2.859	1.263	1.588	1.487
0.05	90	0.00166	348.6	4.358	2.521	1.315	1.436	1.456
0.05	95	0.00168	352.8	4.178	2.238	1.366	1.315	1.419
0.05	100	0.0017	357	4.017	1.999	1.417	1.205	1.386
0.05	105	0.00172	361.2	3.870	1.796	1.468	1.106	1.356
0.05	110	0.00174	365.4	3.737	1.621	1.518	1.017	1.327
0.05	115	0.00176	369.6	3.616	1.470	1.568	0.941	1.297
0.05	120	0.00178	373.8	3.505	1.339	1.618	0.871	1.270
0	125	0.0018	378	3.402	1.224	1.667	1.018	1.215
0.01	130	0.00182	382.2	3.308	1.123	1.717	0.904	1.201
0.02	135	0.00184	386.4	3.220	1.033	1.765	0.805	1.184
0.03	140	0.00186	390.6	3.139	0.954	1.814	0.717	1.166
0.04	145	0.00188	394.8	3.063	0.883	1.863	0.639	1.147
0.05	150	0.0019	399	2.993	0.819	1.911	0.571	1.126
0.06	155	0.00192	403.2	2.927	0.762	1.959	0.509	1.106
0.07	160	0.00194	407.4	2.865	0.711	2.007	0.455	1.085
0.08	165	0.00196	411.6	2.807	0.664	2.055	0.408	1.064
0.09	170	0.00198	415.8	2.752	0.622	2.103	0.366	1.043
0.1	175	0.002	420	2.700	0.584	2.151	0.328	1.023
0.02	100	0.0017	357	4.017	1.999	1.417	1.364	1.353
0.04	100	0.0017	357	4.017	1.999	1.417	1.258	1.375
0.06	100	0.0017	357	4.017	1.999	1.417	1.112	1.418
0.08	100	0.0017	357	4.017	1.999	1.417	1.054	1.420
0.1	100	0.0017	357	4.017	1.999	1.417	0.956	1.444

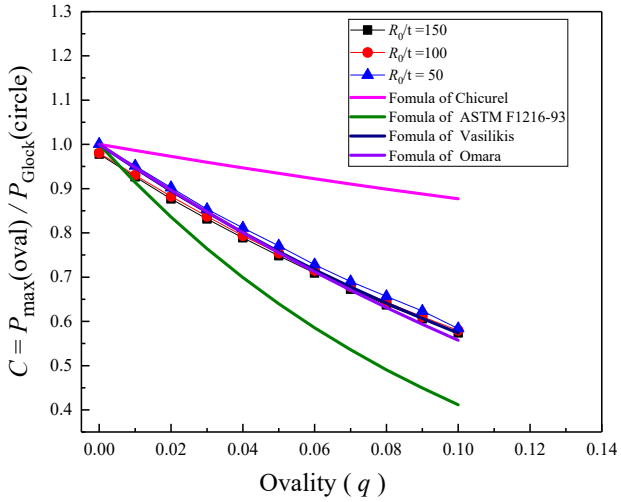

Figure 5. Comparison between finite element calculation results and empirical formula of attenuation coefficient under ovality defect.

Based on the above simulation results, comparing the differences between the sizes of the four attenuation coefficients shown in Table 2 under different ovality defects and the finite element calculation results, as shown in Figure 5, it can be found that the size of *R/t* has a certain impact on the size of $C = \frac{P_{cr}(oval)}{P_{Glcok}(circle)}$, but the impact is relatively low. Although the attenuation coefficient proposed by Khaled M. El-S [28] did not take this factor into account, Khaled M. El-S [28] conservatively takes the lower limit of $\frac{P_{cr}(oval)}{P_{Glcok}(circle)}$ on the *R/t* curve, which makes the calculation results biased towards conservatism. However, overall, the attenuation coefficients related to ovality proposed by Khaled M. El-S [28] and Omara [16] have higher prediction accuracy. Considering that the attenuation coefficient expression proposed by Khaled M. El-S [28] is relatively simple and convenient, this paper intends to refer to the empirical formula for elastic confined buckling of metal liners with ovality defects as shown in Equation (8), providing support for the study of elastic–plastic buckling of metal inner liners in the following text.

$$P_{cr}(oval) = e^{-5.556*q} * \frac{E}{1-\nu^2}\left(\frac{t}{2R}\right)^{2.2} \quad (8)$$

3.2. Nonlinear Confined Buckling Calculation Model of Thin-Walled Metal Liner with Ovality Defects

The elastic confined buckling theory including ovality defects is applicable to metal film liners or plastic liners. In the elastic buckling deformation process of actual metal liners, the Mises equivalent stress of the liner usually exceeds the yield strength of the material and is in a very high stress level state. However, when considering the elasticity and plasticity of the material, the liner will be unstable under lower external pressure, as shown in Figure 6a. For the metal liners with the same structural parameters, When the liner is made of pure elastic material and elastic–plastic material (the yield strength is 310 MPa), the subsequent buckling equilibrium paths are obviously different. The pure elastic material is smoother than the ideal elastic–plastic material at the initial stage of buckling, because the ideal elastic–plastic material produces a plastic hinge at the position where concave buckling occurs, as shown in Figure 6b.

Through the above analysis, it can be found that the nonlinearity of metal liner has a very important influence on the buckling of the liner. At present, it is difficult to obtain its closed analytical formula considering both the nonlinearity of the material and the ovality defect. In light of these complexities, an empirical formula is developed based on finite element simulations, aiming to provide a practical solution for engineering scenarios.

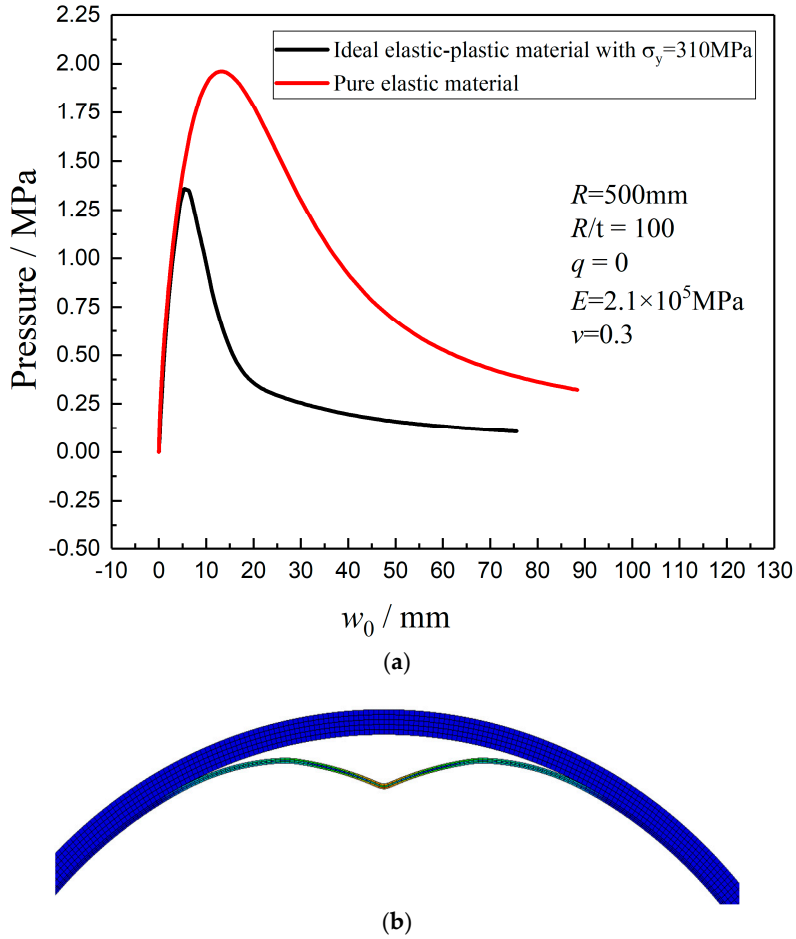

Figure 6. Finite element results of confined buckling. (**a**) Post buckling equilibrium path of elastic–plastic liner and pure elastic liner. (**b**) Plastic hinge.

3.2.1. Criteria for Judging Nonlinear Confined Buckling

In order to study the influence of the nonlinearity of the liner material on the critical buckling pressure, Vasilikis et al. [26] first proposed a parameter λ as shown in Equation (9) to determine the characteristics of the liner: thin-walled liner (elastic instability) and thick-walled liner (plastic instability), where $P_y = 2\frac{\sigma_y}{\sqrt{1-\nu+\nu^2}}\left(\frac{t}{2R}\right)$ is the critical external pressure when the liner yields under external pressure, and the factor $1/\sqrt{1-\nu+\nu^2}$ considers the influence of plane strain conditions on yield strength. Therefore, the parameter λ is determined by the uniaxial tensile yield stress σ_y of the liner material and the diameter–thickness ratio $\frac{R}{t}$ of the liner.

$$\lambda = \sqrt{\frac{P_y}{P_{Glock}}} = \sqrt{\frac{2\sigma_y(1-\nu^2)}{E\sqrt{1-\nu+\nu^2}}\left(\frac{2R}{t}\right)^{1.2}} \tag{9}$$

It can be found that the parameter λ is directly proportional to the $\frac{\sigma_y}{E}$ and $\frac{R}{t}$. For a circular liner without ovality defects, when the $\frac{\sigma_y}{E}$ and $\frac{R}{t}$ of the liner are relatively large, the parameter λ would greater than a certain critical value λ_p, and the liner will probably buckle elastically. At this stage, the critical buckling pressure of the metal liner coincides with Glock's theoretical value ($P_{\mathrm{cr}} = P_{Glock}$). Equation (9) can be reformulated as Equation (10).

$$\frac{P_{\mathrm{cr}}}{P_y} = \frac{1}{\lambda^2},\ (\lambda > \lambda_p) \tag{10}$$

When the liner is elastically buckled and contains initial defects, the critical external pressure of the liner is estimated by using the attenuation coefficient C, as shown in the Equation (11).

$$\frac{P_{\mathrm{cr}}}{P_y} = \frac{C}{\lambda^2},\ (\lambda > \lambda_p) \tag{11}$$

Vasilikis et al. [26] also stipulated that when $\lambda \leq \lambda_0$, the liner will enter the overall yield state, as shown in the Equation (12).

$$\frac{P_{\mathrm{cr}}}{P_y} = 1,\ (\lambda \leq \lambda_0) \tag{12}$$

However, when $\lambda_0 \leq \lambda \leq \lambda_p$, the liner is in the nonlinear buckling stage, which is different from the whole buckling stage. During the nonlinear buckling stage, material points at the liner's buckling location undergo yielding, resulting in a localized stiffness reduction that accelerates the buckling process. Consequently, both the yield stress and the diameter-to-thickness ratio of the liner jointly influence the critical buckling pressure. As nonlinear liner buckling lacks a closed-form solution, the European Committee for Standardization [39] adopted Equation (4).

$$\frac{P_{\mathrm{cr}}}{P_y} = 1 - \beta\left(\frac{\lambda - \lambda_0}{\lambda_p - \lambda_0}\right)^{\eta},\ (\lambda_0 \leq \lambda \leq \lambda_p) \tag{13}$$

Among them, $\beta = 1 - C/\lambda_p^2$ and C are the attenuation coefficients represented by various defects related to the liner. η is a dependent parameter related to the defect size of the liner and the structural parameters of the liner.

For the circular steel liner without defects, Vasilikis et al. [26] have determined the upper and lower limits of the parameter λ related to the nonlinear confined buckling, which are $\lambda_0 = 0.25$ and $\lambda_p = 2.2$, respectively. Since these boundary values have been well-defined in previous work, their derivation is not repeated here. Instead, this study focuses on investigating nonlinear buckling behavior in metal liners with ovality defects, using these established bounds as the basis for analysis.

3.2.2. Calculated Models for Nonlinear Confined Buckling of Metal Liner with Ovality Defects

For metal liners with ovality defects, the condition $0.25 < \lambda < 2.2$ indicates operation within the nonlinear confined buckling regime. Building upon the empirical formulation for nonlinear critical buckling established by the European Committee for Standardization [39], and this chapter develops an enhanced empirical formula incorporating the dependent parameter η as a key factor. Furthermore, we introduce an ovality defect attenuation coefficient to account for geometric imperfections. The resulting empirical formulation for nonlinear confined buckling of ovalized metal liners is presented in Equation (14).

$$C = \frac{P_{\mathrm{cr}}}{P_y} = 1 - \left(1 - \frac{\mathrm{e}^{-5.556*q}}{2.2^2}\right)\left(\frac{\lambda - \lambda_0}{\lambda_p - \lambda_0}\right) * \eta,\ (\lambda_0 \leq \lambda \leq \lambda_p) \tag{14}$$

In Equation (14), the dependent parameter η is the only unknown parameter. Therefore, the finite element model of metal liner is established and the expressions of dependent parameter η about ovality q and liner's structural parameter λ are fitted according to the obtained critical buckling calculation results. Firstly, the expression of dependent parameter η as shown in Equation (15) is obtained by transforming Equation (14). Then, by establishing 36 groups of finite element calculation models as shown in Table 6, the size of dependent parameter η is calculated by Equation (15), where P_{max} represent the maximum

pressure (as exemplified by the peak point in Figure 6a) obtained through Riks analysis in ABAQUS.

$$\eta = \left(1 - \frac{P_{\max}}{P_y}\right) / \left[\left(1 - \frac{e^{-5.556*q}}{2.2^2}\right)\left(\frac{\lambda - 0.25}{2.2 - 0.25}\right)\right] \quad (15)$$

As shown in Table 6, R/t and σ_y/E are two groups of dimensionless data, namely, the specific thickness of metal liner radius and the specific elastic modulus of plastic yield stress. In order to simulate the metal liner with ovality defects, the value range of ovality q is set at 0~0.1.

Through curve fitting, the corresponding coefficient is derived in the form of $\eta = 1/\left(26.42q^2 - 0.01\lambda^2 - 8.56q + 0.16\lambda + 3.38q\lambda + 0.63\right)$. Based on this formulation, the nonlinear buckling external pressure for metal liners with ovality defects can be empirically expressed as given in Equation (16).

$$P_{cr} = \begin{cases} P_y & , \quad \lambda < 0.25 \\ \left[1 - \dfrac{\left(1 - \dfrac{e^{-5.556*q}}{2.2^2}\right)\left(\dfrac{\lambda - 0.25}{2.2 - 0.25}\right)}{26.42q^2 - 0.01\lambda^2 - 8.56q + 0.16\lambda + 3.38q\lambda + 0.63}\right] * P_y & , \quad 0.25 \le \lambda \le 2.2 \\ \dfrac{e^{-5.556*q}}{\lambda^2} P_y & , \quad \lambda > 2.2 \end{cases} \quad (16)$$

In order to test the prediction accuracy of the empirical formula, five groups of finite element calculation models with ovality defects and different parameters λ were established. The parameters of the finite element model, the maximum calculated pressure $P_{\max}$ calculated by Riks analysis step and the predicted result P_{cr} of empirical formula are shown in Table 7. The error between the predicted result and the simulated result of finite element is relatively low, with a maximum of 4.98%. Therefore, the empirical formula shown in Equation (16) can well describe the attenuation of critical buckling pressure caused by structural parameters and ovality defects of the liner.

Table 7. Comparison between prediction results of empirical formula and finite element calculation results.

q	R/t	σ_y/E	σ_y (MPa)	P_y (MPa)	P_{Glock} (MPa)	λ	$P_{\max}$ (MPa)	P_{cr} (MPa)	$\frac{P_{\max}-P_{cr}}{P_{\max}}$
0.05	50	0.0017	357	8.033	9.187	0.935	3.873	3.834	1.00%
0.05	75	0.0017	357	5.355	3.765	1.193	2.004	1.976	1.40%
0.05	100	0.0017	357	4.017	1.999	1.417	1.205	1.177	2.30%
0.05	125	0.0017	357	3.213	1.224	1.620	0.795	0.755	4.98%
0.05	150	0.0017	357	2.678	0.819	1.808	0.524	0.504	3.71%

4. Experimental Validation

4.1. Test Parameters

To validate the proposed nonlinear buckling pressure equation (Equation (16) in Section 3.2.2), this chapter compares and analyzes experimental data from Zhang et al. [27]. Their study investigated the mechanical behavior of thin-walled S30408 stainless steel

liners inside the COPVs, developing a method to calculate the critical internal pressure that prevents liner buckling.

Zhang et al. [27] employed a semi-empirical formula (Equation (4)) originally proposed by Montel [23], which was derived from Timoshenko's thin ring deflection theory [24] and experimental data [25]. However, this formulation only accounts for initial deflection and clearance effects, neglecting the influence of ovality defects on nonlinear confined buckling.

Notably, integrating Zhang et al.'s theoretical approach with the semi-empirical formula proposed in this study enables accurate prediction of critical internal pressures for Type-III COPVs with ovality defects. Their experimental work involved S30408 stainless steel liners wrapped with carbon fiber layers. Through load–unload cycle testing, they observed buckling initiation at 15–18 MPa, characterized by circumferential inward single-wave deformation of the liner.

4.2. Comparison of Experimental and Theoretical Calculation Results

According to the structural parameters of the Type-III COPV described by Zhang [27], the ovality defect of their liner is 0.01. Combined with the empirical calculation formula of critical buckling pressure of metal liner with ovality defect proposed in this paper, as shown in Equation (16), and the calculation method of critical internal pressure when the liner buckled proposed by Zhang. Substituting the parameters of the tested Type-III COPV [27] into the proposed semi-empirical formula of Equation (16), when the liner is subjected to nonlinear confined buckling, the theoretical critical internal pressure is 18.5 MPa, in which the error range of the calculation result based on the semi-empirical formula proposed in this paper is −2.8%~−23%. For comparison, the calculation result of Zhang et al. based on Equation (4) is 4%~20%. The error between the two formulas and the experimental results is shown in Table 8. The error range of the semi-empirical formula based on Equation (16) shows that the prediction result is slightly higher than the tested value. The main reason could be that the metal lining used by the experimental subjects may have other unobserved initial defects, such as initial deflection, uneven wall thickness, etc. Current research [8,13,22,23] indicates that these defects can lead to a reduction in the critical confined buckling pressure of the inner. Nowadays, the coupling mechanism of these defects is not yet clear, but the empirical formula established based on the finite element method in this paper provides a new solution path.

Table 8. Comparison of calculation results of different empirical formulas.

Semi-Empirical Formula	Calculated Results	Errors
Equation (4)	14.4 MPa	4~20%
Proposed formula (Equation (16))	18.5 MPa	−2.8~−23%

Note: Experimental value [27]: 15~18 MPa.

5. Conclusions and Outlook

In this paper, the nonlinear confined buckling pressure of thin-walled metal liner with initial ovality defect is studied through finite element analysis and theoretical derivation. The nonlinear confined buckling pressure of metal liner with ovality defects is discussed by finite element analysis method, and a semi-empirical calculation formula of nonlinear confined buckling pressure of metal liner with ovality defects was established, by 36 sets of parameterized finite element calculation data. The error range between the theoretical prediction results and the experimental results is −2.8~−23%.

The finite element calculation model can perfectly predict the critical pressure of elastic confined buckling. The coupling mechanism of these defects is not yet clear, but the empirical formula established based on the finite element method in this paper provides

a new solution path. In this paper, the finite element calculation model is based on a 2D plane strain model, without fully considering the influence conditions in the axial direction of the liner. Therefore, the finite element calculation results are only applicable to pipelines with a large aspect ratio. For axially discontinuous inner lining structures such as reducers or bends, it is recommended to use a three-dimensional model for calculation.

The fabrication of metal liner test specimens incorporating diverse initial defects, along with real-time monitoring of their buckling behavior, is crucial for validating and refining accurate finite element models. Further investigations are required to systematically address these research gaps.

Author Contributions: Conceptualization, F.G.; Data curation, H.X.; Formal analysis, F.G.; Investigation, F.G., H.W. and Y.J.; Methodology, F.G.; Resources, Z.C. and X.L.; Software, F.G. and K.S.; Supervision, Z.C.; Validation, K.S.; Visualization, H.W. and X.L.; Writing—original draft, F.G. and H.X.; Writing—review and editing, Z.T. All authors have read and agreed to the published version of the manuscript.

Funding: This research was funded by the Postgraduate Practice Innovation Program of Jiangsu University of Technology grant number [XSJCX24_73], the Changzhou Sci&Tech Program grant number [CJ20240029], the Changzhou Leading Talent Program Project of D Category grant number [CQ20240098] and Jiangyin Hengdu Machinery Co., Ltd. Grant number [2024320400002666].

Institutional Review Board Statement: Not applicable.

Informed Consent Statement: Not applicable.

Data Availability Statement: The original contributions presented in this study are included in the article. Further inquiries can be directed to the corresponding author.

Conflicts of Interest: Author Yaguo Jin was employed by the company Jiangsu Ankura intelligent electric Co., Ltd. The remaining authors declare that the research was conducted in the absence of any commercial or financial relationships that could be construed as a potential conflict of interest.

References

1. Zhou, G.; Niu, Y.; Zhao, J.; Wang, Y. Multi-objective optimization design of NPR protection shell for hydrogen storage tank. *Mech. Adv. Mater. Struct.* **2024**, *32*, 1–14. [CrossRef]
2. Ahmad, S.; Ullah, A.; Samreen, A.; Qasim, M.; Nawaz, K.; Ahmad, W.; Alnaser, A.; Kannan, A.M.; Egilmez, M. Hydrogen production, storage, transportation and utilization for energy sector: A current status review. *J. Energy Storage* **2024**, *101*, 113733. [CrossRef]
3. Choi, B.H.; Kwon, I.B. Damage mapping using strain distribution of an optical fiber embedded in a composite cylinder after low-velocity impacts. *Compos. Part B Eng.* **2019**, *173*, 107009. [CrossRef]
4. Jahromi, B.H.; Ajdari, A.; Nayeb-Hashemi, H.; Vaziri, A. Autofrettage of layered and functionally graded metal–ceramic composite vessels. *Compos. Struct.* **2010**, *92*, 1813–1822. [CrossRef]
5. Hu, J.; Chandrashekhara, K. Fracture analysis of hydrogen storage composite cylinders with liner crack accounting for autofrettage effect. *Int. J. Hydrogen Energy* **2009**, *34*, 3425–3435. [CrossRef]
6. Li, C.; Qin, Z.; Li, Y.; Chen, Z.; Liu, J.; Liang, J.; Feng, J. Investigation on mechanical behaviors under fatigue load of stacking sequences considering autofrettage process for highly reliable hydrogen storage vessel. *J. Energy Storage* **2024**, *82*, 110538. [CrossRef]
7. Wu, E.; Zhao, Y.; Zhao, B.; Xu, W. Fatigue life prediction and verification of high-pressure hydrogen storage vessel. *Int. J. Hydrogen Energy* **2021**, *46*, 30412–30422. [CrossRef]
8. Zhang, Q.; Yang, D.; Shen, M.; Li, Z. Analytical and numerical predictions of elastoplastic buckling behaviors of the subsea lined pipelines with ovality defects under hydrostatic pressure. *Thin-Walled Struct.* **2024**, *205*, 112584. [CrossRef]
9. Xia, Y.; Jiang, N.; Yao, Y.; Sun, J.; Zhang, Z. Theoretical and numerical methods for analyzing the dynamic response of buried pipelines under blasting vibrations. *Eng. Fail. Anal.* **2025**, *170*, 109322. [CrossRef]
10. Hongli, D. *Theoretical and Experimental Study on Elastic and Plastic Thermal Buckling of Steel Lining Shell*; Tsinghua University: Beijing, China, 1996.
11. Yingdong, J. *Study on Buckling Behavior of Defective Lining*; China Geo University: Beijing, China, 2016.

12. Guo, Z. *Study on Limited Instability of Thin-Walled Cylindrical Shells*; Fuzhou University: Fuzhou, China, 2013.
13. Yamamoto, Y.; Matsubara, N. Buckling strength of metal lining of a cylindrical pressure vessel. *Trans. Jpn. Soc. Mech. Eng. Ser. A* **1969**, *45*, 421–429. [CrossRef]
14. Yantian, L.; Li, Z. Stability calculation of external pressure cylindrical shell with rigid outer wall. *J. Wuhan Inst. Chem. Technol.* **1991**, 28–35. [CrossRef]
15. Moore, I.D.; Haggag, A.; Selig, E.T. Buckling strength of flexible cylinders with nonuniform elastic support. *Int. J. Solids Struct.* **1994**, *31*, 3041–3058. [CrossRef]
16. Omara, A.-A.M.; Guice, L.K.; Straughan, W.T.; Akl, F. Instability of thin pipes encased in oval rigid cavity. *J. Eng. Mech.* **2000**, *126*, 381–388. [CrossRef]
17. Blanc-Vannet, P.; Papin, P.; Weber, M.; Renault, P.; Pepin, J.; Lainé, E.; Tantchou, G.; Castagnet, S.; Grandidier, J.-C. Sample scale testing method to prevent collapse of plastic liners in composite overwrapped pressure vessels. *Int. J. Hydrogen Energy* **2019**, *44*, 8682–8691. [CrossRef]
18. Rueda, F.; Marquez, A.; Otegui, J.; Frontini, P. Buckling collapse of HDPE liners: Experimental set-up and FEM simulations. *Thin-Walled Struct.* **2016**, *109*, 103–112. [CrossRef]
19. Wang, J.H.; Koizumi, A. Experimental investigation of buckling collapse of encased liners subjected to external water pressure. *Eng. Struct.* **2017**, *151*, 44–56. [CrossRef]
20. Glock, D. Überkritisches verhalten eines starr ummantelten kreisrohres bei wasserdrunck von aussen und temperaturdehnung (post-critical behavior of a rigidly encased circular pipe subject to external water pressure and thermal extension). *Der Stahlbau* **1977**, *7*, 212–217.
21. Boot, J.C. Elastic buckling of cylindrical pipelings with small imperfections subjected to external pressure. *Trenchless Technol. Res.* **1998**, *12*, 3–15. [CrossRef]
22. Li, Z.; Wang, L.; Guo, Z.; Shu, H. Elastic buckling of cylindrical pipe linings with variable thickness encased in rigid host pipes. *Steel Constr.* **2012**, *51*, 10–19. [CrossRef]
23. Montel, R. Formule semi-empirique pour la détermination de la pression extérieure limite d'instabilité des conduites métalliques lisses noyées dans du béton. *La Houille Blanche* **1960**, *46*, 560–568. [CrossRef]
24. Timoshenko, S.P. *Theory of Elastic Stability*; McGraw-Hill: Moscow, Russia, 1936.
25. Borot, M. Essais des Conduits Metálliques Noyées Dans du Béton. *La Houille Blanche* **1957**, *6*, 881–887. [CrossRef]
26. Vasilikis, D.; Karamanos, S.A. Stability of confined thin-walled steel cylinders under external pressure. *Int. J. Mech. Sci.* **2009**, *51*, 21–32. [CrossRef]
27. Zhang, P.; Gu, F.; Cao, Z.; Wang, H.; Chen, Z.; Xiao, H.; Wang, X.; Ma, G. Theoretical and experimental research on the critical buckling pressure of the thin-walled metal liner installed in the composite overwrapped pressure vessel. *Int. J. Press. Vessel. Pip.* **2024**, *212*, 105335. [CrossRef]
28. Elsawy, K.; Moore, I.D. Parametric study for buckling of liners: Effect of liner geometry and imperfections. In *Trenchless Pipeline Projects*; ASCE: Reston, VA, USA, 2014. [CrossRef]
29. Kyriakides, S.; Youn, S.K. On the collapse of circular confined rings under external pressure. *Int. J. Solids Struct.* **2015**, *20*, 699–713. [CrossRef]
30. Lo, K.H.; Zhang, J.Q. *Collapse Resistance Modeling of Encased Pipes*; Shell Development Company: Houston, TX, USA, 1994.
31. Li, J.Y.; Guice, L.K. Buckling of encased elliptic thin ring. *J. Eng. Mech.* **1995**, *121*, 1325–1329. [CrossRef]
32. El-Sawy, K.; Moore, I.D. Stability of loosely fitted liners used to rehabilitate rigid pipes. *J. Struct. Eng.* **1998**, *124*, 1350–1357. [CrossRef]
33. Jaganathan, A.; Allouche, E.; Baumert, M. Experimental and numerical evaluation of the impact of folds on the pressure rating of CIPP liners. *Tunn. Undergr. Space Technol.* **2007**, *22*, 666–678. [CrossRef]
34. El-Sawy, K.M.; Sweedan, A. Effect of local wavy imperfections on the elastic stability of cylindrical liners subjected to external uniform pressure. *Tunn. Undergr. Space Technol.* **2010**, *25*, 702–713. [CrossRef]
35. Vasilikis, D.; Karamanos, S.A. Buckling design of confined steel cylinders under external pressure. *J. Press. Vessel Technol.* **2011**, *133*, 11205. [CrossRef]
36. El-Sawy, K.M. Inelastic stability of liners of cylindrical conduits with local imperfection under external pressure. *Tunn. Undergr. Space Technol.* **2013**, *33*, 98–110. [CrossRef]
37. Chicurel, R. Shrink Buckling of Thin Circular Rings. *J. Appl. Mech.* **1968**, *35*, 608–610. [CrossRef]

38. Plastics, D.O. *Standard Practice for Rehabilitation of Existing Pipelines and Conduits by the Inversion and Curing of a Resin-Impregnated Tube*; ASTM: West Conshohocken, PA, USA, 2024.
39. Rotter, J.M.; Schmidt, H. *European Convention for Constructional Steelwork. Buckling of Steel Shells*; European Design Recommendations; ECCS: Brussels, Belgium, 2008.